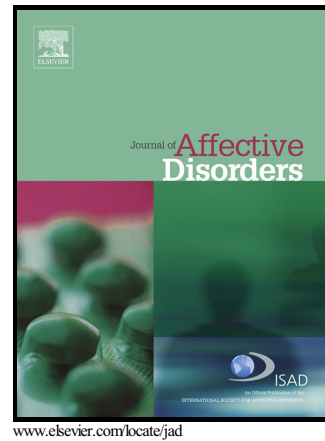


Resting-State Functional Network Connectivity in Prefrontal Regions Differs Between Unmedicated Patients with Bipolar and Major Depressive Disorders

Hao He, Qingbao Yu, Yuhui Du, Victor Vergara, Teresa A. Victor, Wayne C. Drevets, Jonathan B. Savitz, Tianzi Jiang, Jing Sui, Vince D. Calhoun



PII: S0165-0327(15)30153-1
DOI: <http://dx.doi.org/10.1016/j.jad.2015.10.042>
Reference: JAD7812

To appear in: *Journal of Affective Disorders*

Received date: 28 April 2015
Revised date: 6 September 2015
Accepted date: 22 October 2015

Cite this article as: Hao He, Qingbao Yu, Yuhui Du, Victor Vergara, Teresa A. Victor, Wayne C. Drevets, Jonathan B. Savitz, Tianzi Jiang, Jing Sui and Vince D. Calhoun, Resting-State Functional Network Connectivity in Prefrontal Regions Differs Between Unmedicated Patients with Bipolar and Major Depressive Disorders, *Journal of Affective Disorders*, <http://dx.doi.org/10.1016/j.jad.2015.10.042>

This is a PDF file of an unedited manuscript that has been accepted for publication. As a service to our customers we are providing this early version of the manuscript. The manuscript will undergo copyediting, typesetting, and review of the resulting galley proof before it is published in its final citable form. Please note that during the production process errors may be discovered which could affect the content, and all legal disclaimers that apply to the journal pertain.

Resting-State Functional Network Connectivity in Prefrontal Regions Differs Between Unmedicated Patients with Bipolar and Major Depressive Disorders

Hao He^{1,2}, Qingbao Yu¹, Yuhui Du^{1,3}, Victor Vergara¹, Teresa A. Victor⁴, Wayne C. Drevets⁵, Jonathan B. Savitz⁴, Tianzi Jiang⁶, Jing Sui^{1,6*}, Vince D. Calhoun^{1, 2, 7*}

¹ The Mind Research Network & Lovelace Biomedical and Environmental Research Institute, Albuquerque, NM, USA

² Electrical and Computer Engineering Department, University of New Mexico, Albuquerque, NM, USA

³ School of Information and Communication Engineering, North University of China, Taiyuan, China

⁴ Laureate Institute for Brain Research, Tulsa, OK, USA

⁵ Janssen Pharmaceuticals of Johnson & Johnson, Inc., Titusville, NJ, USA

⁶ Brainnetome Center and National Laboratory of Pattern Recognition, Institute of Automation, Chinese Academy of Sciences, Beijing, China

⁷ Department of Psychiatry, Yale University, New Haven, CT, USA

Initial version submitted to Journal of Affective Disorders on Apr 28, 2015

First revised version submitted to Journal of Affective Disorders on July 31, 2015

Second revised version submitted to Journal of Affective Disorders on Sep 5, 2015

Address for Correspondence:

Jing Sui, Vince D. Calhoun
The Mind Research Network,
1101 Yale Blvd, NE,
Albuquerque, NM, 87106
Email: jing.sui@nlpr.ia.ac.cn, vcalhoun@mrn.org

Running Title:

FNC in PFC differs between BD and MDD

Abstract and Keywords

Background: Differentiating bipolar disorder (BD) from major depressive disorder (MDD) often poses a major clinical challenge, and optimal clinical care can be hindered by misdiagnoses. This study investigated the differences between BD and MDD in resting-state functional network connectivity (FNC) using a data-driven image analysis method.

Methods: In this study, fMRI data were collected from unmedicated subjects including 13 BD, 40 MDD and 33 healthy controls (HC). The FNC was calculated between functional brain networks derived from fMRI using group independent component analysis (ICA). Group comparisons were performed on connectivity strengths and other graph measures of FNC matrices.

Results: Statistical tests showed that, compared to MDD, the FNC in BD was characterized by more closely connected and more efficient topological structures as assessed by graph theory. The differences were found at both the whole-brain-level and the functional-network-level in prefrontal networks located in the dorsolateral/ventrolateral prefrontal cortex (DLPFC, VLPFC) and anterior cingulate cortex (ACC). Furthermore, interconnected structures in these networks in both patient groups were negatively associated with symptom severity on depression rating scales.

Limitations: As patients were unmedicated, the sample sizes were relatively small, although they were comparable to those in previous fMRI studies comparing BD and MDD.

Conclusions: Our results suggest that the differences in FNC of the PFC reflect distinct pathophysiological mechanisms in BD and MDD. Such findings ultimately may elucidate the neural pathways in which distinct functional changes can give rise to the clinical differences observed between these syndromes.

Keywords: Bipolar disorders (BD); Major depressive disorder (MDD); Functional network connectivity (FNC); Graph theory; Resting-state fMRI; Brain networks

Highlights

- BD showed more closely connected and efficient functional structures than MDD
- Differences in FNC between BD and MDD were found largely within PFC networks
- More severely depressed patients manifested lower interconnection in PFC networks
- BD exhibited higher clustered FNC in default-mode networks compared to HC
- The difference in FNC between MDD and HC was not significant after FDR correction

1. Introduction

Bipolar disorder (BD) and major depressive disorder (MDD, or unipolar depression) rank among the most debilitating illnesses worldwide (Murray et al., 1996). Both BD and MDD are similarly characterized by depressive episodes, making it difficult to differentiate between the two disorders during the depressed phase (Judd et al., 2003; Judd et al., 2002). BD patients are often misdiagnosed as MDD (Hirschfeld et al., 2003; Hirschfeld and Vornik, 2005), leading to inappropriate and longer medication trials, a poorer prognosis, and greater health care expenses (Dudek et al., 2013; Kupfer, 2005). Objective neuroimaging markers that distinguish BD from MDD may significantly improve diagnostic accuracy, especially in the early phases of the illness (Strakowski et al., 2012), and may thereby facilitate optimal clinical and functional outcome for individuals suffering from either disorder (Cardoso de Almeida and Phillips, 2013). For example, functional magnetic resonance imaging (fMRI) may prove helpful for identifying neurophysiological abnormalities that distinguish BD from MDD. Different patterns of functional activities have been found in BD versus MDD during resting-state or task-based fMRI studies (Almeida et al., 2010; Bertocci et al., 2012; Cerullo et al., 2014; de Almeida et al., 2009; Diler et al., 2013; Taylor Tavares et al., 2008).

Functional connectivity (FC) analysis is an approach that assesses temporal coherence of the hemodynamic activity among brain regions (Friston, 2002). This method is capable of characterizing large-scale integrity of neural activity and provides insight into the functional integration of the brain (Van Dijk et al., 2010). There are two widely used approaches to estimate FC in the brain: regions of interest (ROI) based analysis and independent component analysis (ICA). The ROI-based methods calculate FC between ROIs that are selected based on a prior hypothesis. Although this approach has been widely adopted for the study of mood disorders

(Chepenik et al., 2010; Foland et al., 2008; Raffo et al., 2004; Tang et al., 2013), its efficacy is limited by the variability associated with differences in the shape, size and specific placement of the volumes-of-interest used to extract regional data, as well as by inter-subject anatomical variability (Du et al., 2012; Sui et al., 2009). In contrast, ICA is a multivariate data-driven approach that identifies a set of maximally spatially-independent components (i.e. temporally coherent networks), each with associated time course (Calhoun et al., 2001a, b; Du and Fan, 2013; McKeown et al., 1998; McKeown and Sejnowski, 1998). Without the need of a specific model, ICA is ideal for analyzing resting-state data (Kiviniemi et al., 2003; Sui et al., 2012). Based on the results from ICA, the interrelationship among multiple brain components that can be calculated using pair-wise statistics (i.e. correlations, coherence, etc) between ICA time courses, is defined as functional network connectivity (FNC) (Arbabshirani et al., 2013; Jafri et al., 2008).

Analyses of FC by computing graph theory metrics, such as clustering coefficient, characteristic path length, local efficiency and global efficiency, further assess the topological properties of brain graphs, and provides a useful measure of how effectively information is passed and processed between different brain regions (Rubinov and Sporns, 2010). Graph organizational properties may reveal disease-related abnormalities in functional brain networks among psychiatric patients from resting-state as well as task-related neuroimaging data (He et al., 2012; Lynall et al., 2010; Wang et al., 2010; Yu et al., 2011a; Yu et al., 2011b). However, no previous study has compared the FNC properties between BD and MDD.

The goal of the present study was to investigate the different FNC patterns in BD and MDD patients during the resting-state. We compared connectivity strengths (single-edge weights) and other graph measures of FNC between the two groups. Characterizing how FNC structure

differs in the fMRI data obtained from BD versus MDD samples may increase our understanding of the organization of functional brain networks in these disorders, and may provide potential diagnostic biomarkers to allow for the differentiation of BD from MDD.

2. Materials and Methods

2.1 Subjects

Resting-state fMRI data were collected from 13 BD (Type I: n=7; Type II: n=6), 40 MDD, and 33 age and gender matched HCs at Laureate Institute for Brain Research, Tulsa, OK, USA. The diagnoses of BD and MDD were established using the Structured Clinical Interview for the DSM by trained raters and confirmed by an unstructured interview with a psychiatrist. All patients included in this study were either treatment naïve or had discontinued prescribed medications on their own during at least the 3 weeks (8 weeks for fluoxetine) prior to scanning. No treatment was discontinued for the purposes of the study. The study received institutional ethical review board approval, and all subjects provided written informed consent to participate. The groups did not differ significantly on mean age or gender composition. Symptom severity was assessed using the Montgomery-Åsberg Depression Rating Scale (MADRS) (Montgomery and Åsberg, 1979) and the Young Mania Rating Scale (YMRS) (Young et al., 1978).

At the time of scanning, among the 13 BD subjects, 10 were depressed, one was in a euthymic state, and 2 were in a mixed state. All 40 MDD subjects met criteria for a current major depressive episode and either a recurrent or chronic course.

=====

Insert Table 1 here

2.2 Data acquisition

The data for all three groups were collected with the same time interval (between March 2011 and June 2013). During the fMRI scan, participants were instructed to keep their eyes open in order to prevent sleep. All images were collected on a GE Discovery MR750 3-Tesla scanner with a 32-channel radio frequency coil. T2*-weighted functional images were acquired using a gradient-echo EPI sequence with TE = 27 ms, TR = 2 s, flip angle = 78°, slice thickness = 2.9 mm, field of view = 240 mm, matrix size = 96×96. The resting-state scan lasted 7.5 minutes (225 volumes) for most subjects while some subjects (3 BD, 12 MDD and 10 HC) were scanned for 6.4 min (191 volumes). There was no group effect ($p = 0.87$) with respect to the number of subjects with different scan lengths based on χ^2 analysis.

2.3 Preprocessing

For the fMRI data, the first seven volumes were excluded from analysis to allow for T1 equilibration. The remaining 218 or 184 volumes (depending on scan length) were included in the analysis, and FNC was computed for each subject as the temporal correlations between time course pairs (see Section 2.5). Post hoc tests showed that the relatively small difference in scanning time lengths between subjects did not significantly affect the group analysis, as described below. The SPM8 software package (<http://www.fil.ion.ucl.ac.uk/spm/software/spm8>) was employed to perform fMRI preprocessing. The images were first realigned using INRIalign (Freire et al., 2002), and then were spatially normalized to the standard Montreal Neurological Institute (MNI) space, resampled to 3 mm × 3 mm × 3 mm voxels using the nonlinear (affine +

low frequency direct cosine transform basis functions) registration implemented in SPM8 toolbox. The image data were smoothed using a Gaussian kernel with a small full-width at half-maximum of 8 mm.

Head motion parameters derived from registration were evaluated using four measures (Mean Motion, Maximum Motion, Number of Movements and Mean Rotation) introduced in (Van Dijk et al., 2012). No significant group effect was exhibited using analysis of variance (ANOVA) (see Table S1 in supplementary materials for details).

2.4 Group ICA and post-processing on functional data

Group ICA was performed on the fMRI data using GIFT software (<http://mialab.mrn.org/software/gift>) (Calhoun and Adali, 2012). Individual fMRI images were decomposed via principal component analysis (PCA), with the first 100 components selected for dimension reduction (Allen et al., 2011; Erhardt et al., 2011; Yu et al., 2011a). The infomax algorithm (Bell and Sejnowski, 1995) was repeated 10 times using ICASSO (<http://www.cis.hut.fi/projects/ica/icasso>) to improve the reliability of the decomposition, result in 75 group independent components. Time courses (TCs) and spatial independent components (ICs) of individuals were then back-reconstructed (Calhoun et al., 2001a; Erhardt et al., 2011).

Similar to the IC selection procedures described in (Allen et al., 2011; Damaraju et al., 2014), we generated a one-sample t-test map for each spatial map across all subjects, and thresholded the map to obtain regions of peak activation clusters for each IC. The mean power spectra of the corresponding TCs from each IC were also calculated. The intrinsic connectivity networks (ICNs) were identified if they exhibited peak activations in grey matter, and also showed low spatial overlap with known vascular, ventricular, motion, edges, and susceptibility

artifacts according to the thresholded t-test maps. We additionally ensured that the mean spectral powers of ICNs were dominated by low-frequency fluctuations (Cordes et al., 2000). Forty-eight ICs were characterized as ICNs, while 27 ICs were attributed to physiological, movement related, or imaging artifacts. As remaining noise effects like heart beat and respiration, especially head motion artifact has been reported on connectivity analysis (Power et al., 2012; Van Dijk et al., 2012; Yan et al., 2013), related TCs underwent additional post-processing to remove them (Allen et al., 2014), including 1) detrending linear, quadratic, and cubic trends, 2) multiple regression of the 6 realignment parameters and their temporal derivatives, 3) removal of detected outliers (despiking along each TC), and 4) low-pass filtering with a cutoff of 0.15 Hz.

2.5 FNC Analysis

For each subject, an FNC matrix was calculated using the absolute values of Pearson's correlation between TCs of each pair of 48 ICNs. P-values of corresponding correlation coefficients also were obtained for further analysis. The FNC matrices were then normalized into z-scores using Fisher r-to-z transformation, in order to induce normality on the correlation coefficients. One 48×48 symmetric FNC matrix was obtained for each subject, with entry of element (i, j) corresponding to the strength (or weight) of connectivity between ICNs i and j. The network connectivity strength (Lynall et al., 2010) was specified as absolute z-scores. FC-of-interest were then selected based on p-values obtained from Pearson's correlation with corresponding $p < 0.05$ (2-tailed, uncorrected) in more than 80% of subjects in any one of three groups. An identical overall FC-of-interest pattern was maintained across all subjects for comparison. With non-FC-of-interest entries set to zero, 398 significant connectivity strengths (sparsity at $398 \div 1128 = 35.3\%$) in each FNC matrix were retained for further testing. This sparsity value falls within a range that is not only biologically plausible (Sporns, 2011), but also

proved to keep graph structure reliable (Dennis et al., 2012). Two types of analysis were performed on the FNC matrices: a connectivity analysis and a graph analysis.

2.5.1 Connectivity analysis

Connectivity analysis was performed on the elements of FNC metrics (i.e. strengths of the FC between ICN pairs). ANOVA across groups was performed simultaneously on each FC strength to assess the significance of group effects¹. Two-sample t-tests were then applied to assess the significance of pair-wise group differences² in connectivity for contrasts in which $p < 0.05$ from ANOVA. Please refer to supplemental material S3 for detailed background on the statistical tests. The false discovery rate (FDR) correction (Benjamini and Hochberg, 1995) for multiple testing was applied to the p-values obtained from the statistical tests made on 398 individual FC strengths. Pearson's correlations were used to evaluate relationships between the symptom rating scale scores (MADRS in both BD and MDD subjects) and FC strengths that differed between groups.

2.5.2 Graph analysis

In graph-theory based analyses, FNC were normalized (FC strengths were linearly rescaled into [0, 1] with a uniform factor in all FC strengths across all subjects) and treated as weighted graphs. In the graphs, ICNs correspond to nodes, and the weights of edges linking nodes-pairs are the FC strengths. Within each graph, three nodal metrics including strength, clustering coefficients, and local efficiency were estimated at the functional-network-level (micro-level) for each of 48 nodes. At the same time, four graph metrics including averaged

¹ ANOVA was applied to test whether the population means of the measure (i.e., FNC strength) in the three diagnostic groups were equal based on the sample means of the same measure.

² Two-sample t-tests were performed to evaluate whether the population means of the measure in certain diagnostic group pairs differed significantly based on the measure on samples.

clustering coefficients, characteristic path lengths, global efficiency and averaged local efficiency were evaluated for each brain graph as a whole at the macro-level. The brain connectivity toolbox (<http://sites.google.com/site/bctnet/>) was utilized for the graph metrics computation. Detailed definitions of and formula for these graph metrics can be found in (Rubinov and Sporns, 2010). On nodal graph metrics, significance of group effects were first computed using ANOVA. Nodes with $p < 0.05$ underwent post-hoc t-tests to examine the significance of contrasts between group pairs. The p-values from statistical tests made on 48 individual nodal metrics were corrected using FDR. On global brain graph measures, statistical significance of both group effects and pair-wise group contrasts were tested using ANOVA and t-tests respectively. Correlation between symptom rating scale scores (MADRS in both BD and MDD groups) and graph metrics that showed group differences were evaluated. The BrainNet Viewer toolbox (<http://www.nitrc.org/projects/bnv/>) was used for visualization (Xia et al., 2013).

3. Results

3.1 Group ICA and FNC

Figure 1a displays the spatial maps of 48 ICNs identified from group level ICA. Based on their anatomical and presumed functional properties, 48 ICNs are arranged into groups of auditory (AUD), somatomotor (SM), visual (VIS), cognitive control (CC; putatively referring to the planning, monitoring, and adapting one's behavior), default-mode (DM), and cerebellar (CB) components. ICNs were similar to those observed in previous high model order ICA decompositions (Abou-Elseoud et al., 2010; Allen et al., 2014; Allen et al., 2011; Kiviniemi et al., 2009; Sui et al., 2014). Figure 1b shows the averaged FNC in each group, FNC was averaged

over all subjects and inverse Fisher transformed ($r = \tanh(z)$) back to correlation coefficient for display, facilitating comparisons with previous studies. Overall, BDs showed stronger FC strengths, while strengths in MDDs were slightly weaker.

=====

Insert Figure 1 here

=====

From ANOVA, strong group effects were found in two FC strengths after FDR correction, as displayed in Figure 2: FC strengths between inferior frontal and anterior cingulate cortex (ICN59 – ICN61, $p = 4.50 \times 10^{-4}$), and between left inferior parietal lobule and precentral gyrus (ICN3 – ICN41, $p = 4.46 \times 10^{-4}$). However, both FC only passed FDR at $q = 0.1$, but did not achieve statistical significance after correction at $q = 0.05$. Based on group-pair comparison of FC strengths, two sample t-tests revealed that six FC strengths were either strongly or significantly differentiating between BD and MDD, and another FC strength differed between MDD and HC.

Compared to MDD, BD showed significantly stronger FC strengths within dorsolateral prefrontal (DLPFC) and ventrolateral prefrontal (VLPFC) areas (2 FC strengths, ICN14 – ICN32 $p = 1.82 \times 10^{-4}$, and ICN6 – ICN32, $p = 4.77 \times 10^{-4}$, both FDR corrected), between left postcentral and cuneus (ICN17 – ICN46, $p = 2.84 \times 10^{-4}$, FDR corrected), as well as inferior frontal/ DLPFC to anterior cingulate cortex (ACC) (ICN59 – ICN61, $p = 3.24 \times 10^{-4}$, FDR corrected). Two more FC displayed higher strengths in BD than MDD, including lingual/cuneus to superior temporal (ICN22 – ICN25, $p = 9.16 \times 10^{-4}$) and medial frontal and superior frontal regions (ICN32 –

ICN75, $p = 9.82 \times 10^{-4}$), which approached but did not achieve significance after correction (passed FDR at $q = 0.1$ only, but did not at $q = 0.05$).

Compared to HCs, weaker FC strengths were found in MDD from left inferior parietal lobule to precentral gyrus (ICN3 – ICN41, $p = 1.30 \times 10^{-4}$). However, this difference in FC strengths was reduced to a non-significant trend after correction for multiple testing.

=====

Insert Figure 2 here

=====

3.2 Graph analysis on FNC

A summary of ICNs (nodes) with significant group difference and group effects on nodal graph measures are listed in Table 2 and highlighted in Figure 3.

As shown in Figure 3a, significant group effects from ANOVA existed in nodal strength of ICN67 after FDR correction. The t-tests show five networks, including ICNs lie in DLPFC, VLPFC, ACC and inferior parietal area, were significantly higher ($p < 0.05$, FDR corrected) in nodal strengths in BD than MDD. No significant differences are found between patients and controls.

Figure 3b displays the networks with significant group effects and group difference in clustering coefficients. Five ICNs showing significant group effect ($p < 0.05$, FDR corrected) from ANOVA, which were mostly concentrated in prefrontal regions. In t-tests, three ICNs indicated stronger clustering in BD than HC after FDR correction. A total of fourteen ICNs

distinguished BD from MDD, which lie in frontal, ACC, posterior cingulate cortex (PCC), superior temporal, and parahippocampal areas.

For local efficiency, significant group effect ($p < 0.05$, FDR corrected) on local efficiency was found in ICN67 again from ANOVA test. Seventeen ICNs demonstrated significantly ($p < 0.05$, FDR corrected) higher values in BD comparing to MDD after correction, including ICNs in pre- and mid-frontal, ACC, PCC, superior temporal, cuneus and parahippocampal areas (Figure 3c).

=====

Insert Figure 3 here

=====

=====

Insert Table 2 here

=====

For ANOVA on global brain graph metrics, local efficiency showed significant group effect ($p = 0.0376$), while p-values of clustering coefficient ($p = 0.0513$), characteristic path lengths ($p = 0.0568$) and global efficiency ($p = 0.0901$) were also small but only marginally significant. Between group pairs, despite the fact that no significant group differences were revealed for the graph metrics between patients and HC, all four global brain graph metrics showed differences between BD and MDD (Figure 3d). Compared to MDD, BD showed significantly higher values in clustering coefficient ($p = 0.0099$), global efficiency ($p = 0.0206$)

and local efficiency ($p = 0.0066$), as well as significantly shorter characteristic path lengths ($p = 0.0062$) across the whole brain, indicating the higher efficiency in topology structure of BD.

3.3 Correlation with Symptom Scores

No significant correlations with symptom scores were found in individual FC strengths and global graph measures.

In contrast, the nodal graph measures of the ICNs that located in the DLPFC, ACC, inferior parietal, and parahippocampal cortex regions were negatively correlated ($p < 0.05$, uncorrected) with MADRS scores in both the BD and MDD groups (Table 3). Figure 4 shows a typical network (ICN16) with the overall trends between nodal strength and symptom scores. In the patients with higher MADRS scores the overall nodal connectivity strength, nodal clustering coefficient and nodal local efficient of the ICNs were lower in these brain networks.

=====

Insert Table 3 here

=====

=====

Insert Figure 4 here

=====

4. Discussion

In this study, we used ICA, a data-driven method to separate resting-state fMRI data into ICNs, and built the whole brain functional graph, in which the FNC strengths and its graph measures were computed. We observed that, compared to the MDD group, the FNC of the BD group exhibited higher FC strengths and also was characterized by more efficient topological structures based on measures obtained using graph theory at the functional-network-level in prefrontal cortex as well as at the whole-brain-level. In particular, our findings revealed that the FC strengths and corresponding graph structures which differentiate BD and MDD were mainly located in prefrontal networks including the DLPFC and VLPFC as well as ACC, which is consistent with findings in (Jie et al., 2015). Greater depressive symptom severity correlated with less interconnected structure in prefrontal cortical areas in the patients from both the BD and MDD groups. Although the correlations did not remain significant after correction for multiple comparisons, the trend indicates the potential linkage between altered FC patterns in those ICNs and clinical symptom scores.

Several ICNs implicated in the pathophysiology of mood disorders (e.g., involving functional interactions between prefrontal, anterior cingulate, parahippocampus, cuneus, temporal, parietal, and occipital cortices) were significantly different in FC between the BD and MDD groups. Pair-wise comparisons show that relative to the MDD group, the BD group had significantly stronger FNC strengths within the prefrontal cortex, between the prefrontal cortex and anterior cingulate cortices, cuneus and temporal regions. The prefrontal regions, including the orbitofrontal cortex (OFC), ACC, dorsomedial prefrontal cortex (DMPFC), DLPFC and VLPFC, have been most consistently implicated in cognitive control processes (Sui et al., 2015), including decision-making and emotion regulation (Kupfer et al., 2012; Phillips et al., 2008). Specifically, the ACC and other medial prefrontal areas play major roles in processing emotion

and in automatic or implicit regulation of emotion, whereas lateral prefrontal cortical systems like the DLPFC and VLPFC are implicated in cognitive control and voluntary or effortful regulation of emotion (Drevets, 2001; Phillips et al., 2008). The DLPFC and VLPFC constitute of the limbic-cortical-striatal-pallidal-thalamic circuit system that has been hypothesized to be dysfunctional in mood disorders based on neuroimaging studies (Drevets, 2000; Price and Drevets, 2012). Another study employing effective connectivity analyses (Stein et al., 2007) to examine neural activity in response to fearful and angry faces in healthy subjects found an information-processing path from OFC to DLPFC. Recently, ACC and medial PFC regions have been recognized as part of a neural subcircuit involved in a process with recursive self-focused thinking that leads to negative mood, i.e. rumination (Cooney et al., 2010), which may associate with both BD and MDD (Johnson et al., 2008). Furthermore, it has been reported consistently that the DLPFC and VLPFC are not functioning efficiently towards negative emotions in BD (Brotman et al., 2007; Pavuluri et al., 2007; Pavuluri et al., 2008). These findings are consistent with our results on FNC and symptoms, where significant negative correlations were found between depressive symptom scores and the level of interconnected structure in prefrontal areas in both BD and MDD patients.

The networks of strongest connectivity in the BD group were present in the DLPFC and VLPFC (i.e. ICN6, ICN14, ICN16, and ICN32). The increased FNC indicates possible stronger phase coherence in these ICNs in BD than MDD patients. As reported in electroencephalogram (EEG) studies (Spencer et al., 2004; Varela et al., 2001), phase synchrony has been related to the integrity of the circuits between two brain regions, that is, if two brain regions are locked in phase with each other, their functioning is closely connected. The significantly different FC strengths and local graph measures in the prefrontal ICNs, as well as those in the ACC, PCC,

superior temporal, and parahippocampal areas that consist of the fronto-limbic circuitry between BD and MDD, which implicate the underlying cognitive and mood control schemes are distinct from each other.

Similar findings have been reported by other studies. A low frequency resting-state fMRI study revealed higher correlations between left and right VPFC in BD (Chepenik et al., 2010). Another ICA-defined FNC analysis reported the BD group shows increased connectivity in emotion evaluation regions such as bilateral medial PFC, and in “affective working memory network” including the DLPFC and VLPFC, during an affective working memory task (Passarotti et al., 2012). Abnormal medial PFC connectivity between ICA components were also found during resting-state in the BD group (Calhoun et al., 2011; Ongur et al., 2010; Sui et al., 2011). Decreased blood flow and metabolism in the DMPFC and DLPFC in MDD group have been reported in multiple studies (Baxter et al., 1989; Bench et al., 1992; Drevets, 2000). Compared to BD, (Taylor Tavares et al., 2008) found the MDD group failed to recruit the VLPFC and DMPFC during behavioral reversal learning task that required subjects to ignore misleading negative feedback.

Topologically, clustering coefficients are equivalent to the fraction of the node’s neighbors that are also connected with each other (Watts and Strogatz, 1998). This metric reveals the capacity for specialized processing to occur within densely interconnected brain region groups (Rubinov and Sporns, 2010). Local efficiency reflects the fault tolerance of the graph system, or the efficiency of communication between the first neighbors of a node when it is removed (Latora and Marchiori, 2001). The significantly higher clustering coefficients in the BD group relative to the MDD and HC groups indicate that the ICNs in default-mode nodes including the DLPFC, superior frontal gyrus (SFG) and ACC exhibit stronger local functional

interconnections, and thus potentially showed greater efficiency for local information transfer in those regions in the BD group relative to the other groups. Abnormal function in default-mode networks have been documented in a previous study (Ongur et al., 2010), suggesting abnormal functional organization of neural circuits within BD. At the same time, lower local efficiency in these brain areas suggest that the MDD participants had lower fault tolerance (i.e., more vulnerable) locally compared to BD. However, lower efficiency in frontal cortex may relate to more depressive symptoms, as several networks showed a negative correlation between MADRS and nodal graph measures like strength, clustering coefficient and local efficiency.

The graph metrics at the whole brain level are the averaged metrics across all nodes. Although only a few local ICNs that have significant differences between BD and MDD, which are mostly in prefrontal regions, the averaged metrics shows the same trend. This indicates those graphs are the most influential to the overall brain graph in our study.

With respect to global measures, compared to MDD, FNC in BD had higher global efficiency and shorter characteristic path length. The identified paths show potential routes of information flow between pairs of brain regions (Rubinov and Sporns, 2010). Characteristic path length is a measurement of the extent of average connectivity or the overall routing efficiency of the graph. Shorter path lengths between nodes have also been shown to promote effective interactions across different cortical regions (Achard and Bullmore, 2007). Global efficiency of a graph system is the efficiency of the parallel system, where all the nodes in the graph exchange information concurrently (Abou-Elseoud et al., 2010). According to explanations from (Kaiser and Hilgetag, 2004), ICNs in BD, which have shorter characteristic path length and high global efficiency, are of significance in minimizing noise, shortening signaling delay and increasing synchrony.

Although our study emphasized the identification of differences between BD and MDD, it worth noting that among those comparisons from both FC strengths and graph measures, the most significant group differences occurred between the BD and MDD groups, with weaker contrasts between each mood disorder groups relative to the HC group. Regarding the contrasts between the MDD and HC groups, although the trend of reduced FNC in many brain regions in MDD is consistent with previous literature (Anand et al., 2005a, b; Veer et al., 2010; Wang et al., 2012; Zhu et al., 2012), the group differences reported here were not significant after correction for multiple comparisons. Possibly the high order (number of ICs) ICA model we applied to the whole brain analysis reduced statistical sensitivity by requiring corrections for a relatively large number of comparisons. Notably, a similar result was reported in another study on resting-state FC differences between MDD and HC (Craddock et al., 2009), where no statistical group difference was evident after applying corrections for multiple testing. As shown from the bar plots of graph measures in both whole-brain-level and functional-network-level in various ICNs, BD and MDD were far from each other, with HC in the middle. This overall trend showing HC in between BD and MDD were also found in studies on BOLD responses to positive and negative stimuli (Diler et al., 2013; Grotegerd et al., 2014).

Note that there was a modest variation in the scanning duration across subjects (191 or 225 volumes) although each scan length was similarly represented within each diagnostic group and the mean scan length did not differ significantly across groups. We included all time points available during computation of the temporal correlations. An alternative method is to involve truncation of the longer time courses to match the duration of the shorter ones (keeping only 184 time points for all subjects). However, this step may result in the loss of information. Nevertheless, we retested FNC built from first 184 time points in all subjects, the group

differences still exist in most measures with p-value changed, with several FC strengths and nodal measures failed to pass FDR correction at $q = 0.05$. In addition, we also checked the correlations between the scan durations and reported FNC measures (FC strengths and graph measures) that demonstrated group differences. No significant correlation was found, indicating the relatively small difference in scanning duration did not have a major effect on our results.

Several experimental and methodological issues in our study design merit comment. The major limitation was the small sample size, especially in the BD group. To reduce the potential confound of medication, our study was limited to subjects who were treatment-naïve or unmedicated for at least three weeks, which constrained the patient pool. Nevertheless, most recent neuroimaging studies reviewed in (Cardoso de Almeida and Phillips, 2013) also included sample sizes ranging from 10 to 30 subjects per patient group. It would be helpful to increase statistical power by including more subjects in future studies. In order to maximize the sample size, we included two BD subjects in mixed states and one in a euthymic state, which may have increased the variability of the fMRI data. Consequently, we performed a post hoc analysis to compare the depressed MDD patients versus only the 10 depressed BD subjects, and results were essentially the same as those reported in the original analysis: the group differences still existed although the p-values increased nominally. Further studies may address this limitation by recruiting more specific and clinically matched subjects. Another methodological limitation is that we characterized FNC as the correlation between ICN TCs, rather than use non-linear metrics, such as mutual information, or coherence. While the use of correlation restricts the detection of nonlinear dependencies and the resolution phase of and spectral relationships, this approach is preferred for its straightforward interpretation and tractability. Nevertheless different

connectivity computation methods may be applied in future studies of FNC to gain additional information.

In conclusion, our results show distinct functional network connectivity underlying BD and MDD during resting-states. Overall brain graphs were more topologically efficient in BD than in MDD. The FC strengths and FNC graph metrics that differentiate BD and MDD existed predominantly in prefrontal networks including DLPFC, VLPFC and ACC, which play roles in cognitive control of emotional processing and in other aspects of emotional and visceromotor modulation. These findings raise the possibility that distinct mood control schemes exist between these mood disordered subgroups, which ultimately may be used to guide future studies aimed at differentiating MDD and BD on the basis of biomarkers.

Acknowledgements

This work is supported in part by the National Institute of Biomedical Imaging and Bioengineering (1R01EB006841 to Calhoun, VD), the National Institute of General Medical Sciences Center of Biomedical Research Excellence (COBRE) grant (P20GM103472 to Calhoun, VD), the “100 Talents Plan” of the Chinese Academy of Sciences (to Sui, J), the Chinese Natural Science Foundation (No. 81471367 to Sui, J), the State High-Tech Development Plan of China (863) (Grant No. 2015AA020513 to Sui J), William K. Warren Foundation (to Savitz, JB and Victor, TA), and National Institute of Mental Health (K01MH096077 to Savitz, JB).

Figure Legends

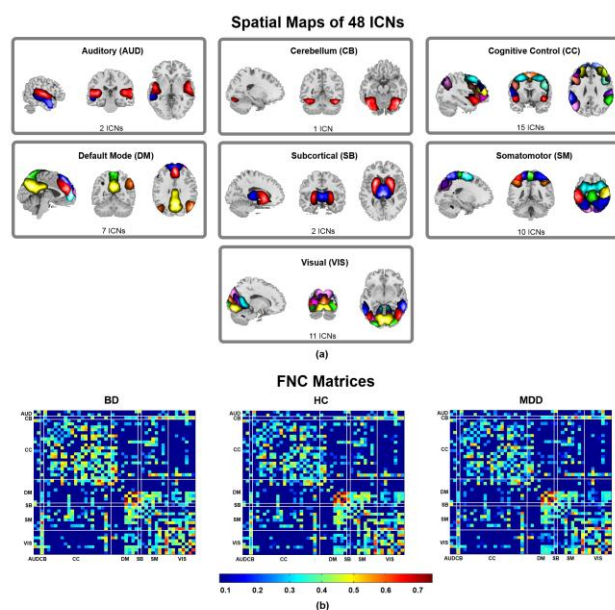


Figure 1. (a) Spatial maps of 48 ICNs and (b) the FNC (correlation matrices) in each group. ICNs are arranged into six categories based on their anatomical and functional properties. FC strengths are averaged over all subjects in each group. (AUD: auditory; CB: cerebellar; CC: cognitive control; DM: default mode; SB: subcortical; SM: somatomotor; VIS: visual)

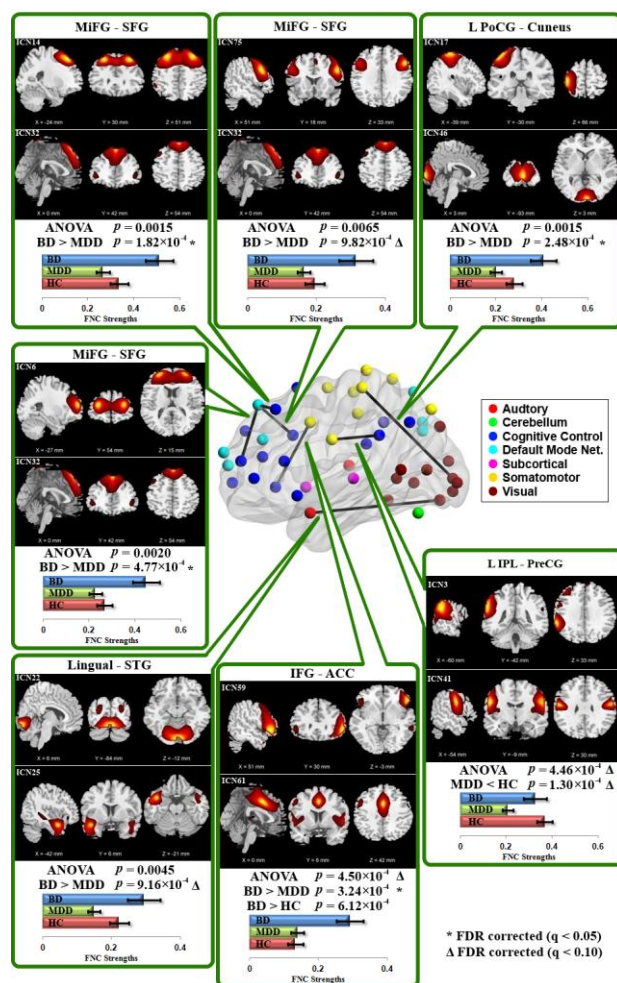


Figure 2. The seven FC strengths differentiated the three groups by statistical tests. The FC strengths highlighted showed both strong ($p < 0.05$) group effects in ANOVA and either significant ($q < 0.05$, FDR corrected) or marginal ($q < 0.1$, FDR corrected) group differences from two-sample t-tests. Dots in the center brain map represent ICNs, and are located at the peak activation points in the brain of corresponding ICNs. Colors of dots correspond to the ICN's anatomical and functional categories. (ACC: anterior cingulate cortex; IFG: inferior frontal gyrus; IPL: inferior parietal lobule; MiFG: middle frontal gyrus; PoCG: postcentral gyrus; PreCG: precentral gyrus; SFG: superior frontal gyrus; STG: superior temporal gyrus)

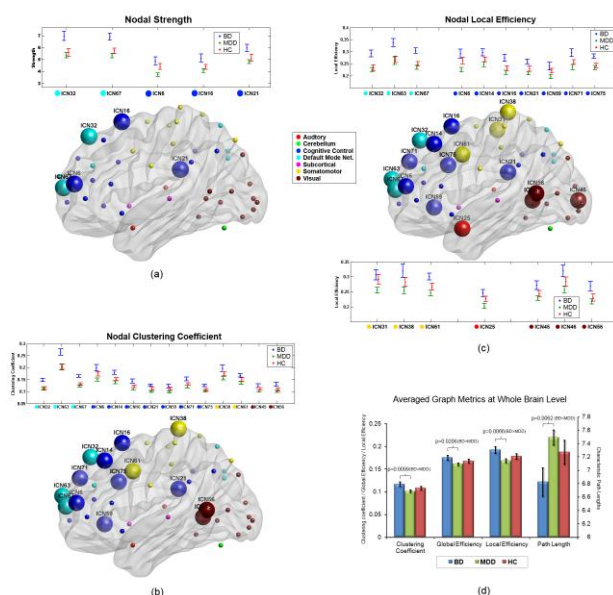


Figure 3. The measures of (a) nodal strength, (b) nodal clustering coefficient, (c) nodal local efficiency, and (d) averaged global graph measures at whole brain level that differentiated the diagnostic groups. For the nodal measures, only ICNs that showed both strong group effects ($p < 0.05$) from ANOVA and significant group differences ($q < 0.05$, FDR corrected) from t-tests are shown in the error bar plots, and highlighted in the brain maps. Dots in the brain maps represent ICNs, and are located at the peak activation points in the brain of corresponding ICNs. Colors of dots correspond to the ICN's anatomical and functional categories. (a) Nodal strengths in 5 ICNs differentiated BD and MDD. (b) Nodal clustering coefficient in 14 ICNs that differentiated BD and MDD, and those in 3 ICNs in default-mode network also significantly different in the BD and HC group. (c) Nodal local efficiency in 17 ICNs differentiated BD and MDD. (d) In global graph metrics at whole brain level, all significant differences were exhibited between BD and MDD, with the measures on the HC group in the middle.

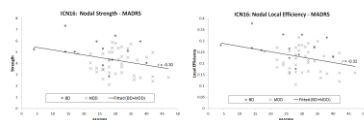


Figure 4. Negative correlations between nodal graph measures (nodal strength and nodal local efficiency) and depressive symptoms scores (MADRS) in patients from both the BD and MDD groups at a typical ICN in DLPFC (ICN16). The more severely depressed, patients showed the lower interconnection around ICN16 were indicated in patients.

Tables

Table 1. Demographic and clinical characteristics of the subject samples

	BD	MDD	HC	p-value
N (Females)	13 (11)	40 (33)	33 (22)	0.22 (chi-square)
Ages	35.15 ± 10.29	35.20 ± 9.31	33.70 ± 10.15	0.84 (ANOVA)
YMRS	6.15 ± 6.11	3.59 ± 2.33	0.16 ± 0.51	<0.001 (ANOVA)
MADRS	24.92 ± 10.31	30.90 ± 6.31	0.73 ± 1.72	<0.001 (ANOVA) 0.0151 (t-test, BD-MDD)

BD: bipolar disorder group; MDD: major depressive disorder group; HC: healthy controls group.

YMRS: Young Mania Rating Scale; MADRS: Montgomery-Åsberg Depression Rating Scale.

Table 2. ICNs with Group Differences / Group Effect in Nodal Metrics

ICN	Peak Coordinate X,Y,Z (mm)	Nodal Strength		Nodal Clustering Coefficient			Nodal Local Efficiency	
		P _{ANOVA}	P _{BD-MDD}	P _{ANOVA}	P _{BD-MDD}	P _{BD-HC}	P _{ANOVA}	P _{BD-MDD}
Auditory								
Parahippocampal (ICN25)	-42,6,-21						0.0174	0.0116*
Cognitive Control								
DLPFC/ACC (ICN6)	-27,54,15	0.0048	0.0011*	0.0030*	0.0005*		0.0042 ^Δ	0.0010*
DLPFC (ICN14)	-24,30,51			0.0028*	0.0011*		0.0218	0.0011*
DLPFC (ICN16)	0,15,66	0.0155	0.0038*	0.0075 ^Δ	0.0016*		0.0042 ^Δ	0.0009*
IPL (ICN21)	63,-33,27	0.0272	0.0008*	0.0047*	0.0001*		0.0127	0.0005*
MiFG (ICN59)	51,30,-3			0.0142 ^Δ	0.0096*		0.0299	0.0183*
DLPFC (ICN71)	30,51,36			0.0109 ^Δ	<0.0001*		0.0127	0.0060*
DLPFC (ICN75)	51,18,33			0.0187 ^Δ	0.0034*		0.0302	0.0060*
Default Mode								
DLPFC/VLPFC (ICN32)	0,42,54	0.0080	0.0009*	0.0013*	0.0001*	0.0030*	0.0032 ^Δ	0.0004*
SFG (ICN63)	15,66,21			0.0172 ^Δ	0.0084*	0.0023*	0.0274	0.0162*
SFG/ACC (ICN67)	0,63,12	0.0005*	0.0001*	0.0002*	0.0128*	0.0009*	0.0004*	0.0001*
Somatomotor								
R PoCG (ICN31)	45,-24,63						0.0409	0.0121*
MiFG (ICN38)	0,-33,78			0.0209 ^Δ	0.0064*		0.0188	0.0055*
ACC (ICN61)	0,6,42			0.0287 ^Δ	0.0185*		0.0194	0.0039*
Visual								
PCC/ Parahippocampal (ICN45)	-6,-54,3			0.0306 ^Δ	0.0047*		0.0418	0.0078*
Cuneus (ICN46)	3,-93,3						0.0343	0.0069*
STG (ICN56)	-57,-57,9			0.0195 ^Δ	0.0026*		0.0343	0.0058*

^Δ FDR corrected with $q < 0.10$ * FDR corrected with $q < 0.05$

BD: bipolar disorder group; MDD: major depressive disorder group; HC: healthy controls group.

ICN: intrinsic connectivity network. ACC: anterior cingulate cortex; DLPFC: dorsolateral prefrontal cortex; IPL: inferior parietal lobule; MiFG: middle frontal gyrus; PCC: posterior cingulate cortex; IPL: inferior parietal lobule; SFG: superior frontal gyrus; STG: superior temporal gyrus; VLPFC: ventrolateral prefrontal cortex.

Table 3. Significant Correlations in Patient Groups between Nodal Metrics and Depression Rating Scale (MADRS)

ICN	Peak Coordinate X,Y,Z (mm)	Nodal Strength	Nodal Clustering Coefficient	Nodal Local Efficiency
Auditory				
Parahippocampal (ICN25)	-42,6,-21			r = -0.3605 p = 0.0080
Cognitive Control				
DLPFC (ICN16)	0,15,66	r = -0.3009 p = 0.0286	r = -0.2971 p = 0.0307	r = -0.3184 p = 0.0202
IPL (ICN21)	63,-33,27		r = -0.2949 p = 0.0321	r = -0.2750 p = 0.0462
DLPFC (ICN71)	30,51,36		r = -0.2833 p = 0.0398	r = -0.2920 p = 0.0339
Somatomotor				
R PoCG (ICN31)	45,-24,63			r = -0.2753 p = 0.0460
ACC (ICN61)	0,6,42		r = -0.2919 p = 0.0339	r = -0.3605 p = 0.0080

ICN: intrinsic connectivity network. ACC: anterior cingulate cortex; DLPFC: dorsolateral prefrontal cortex; IPL: inferior parietal lobule; IPL: inferior parietal lobule.

References

- Abou-Elseoud, A., Starck, T., Remes, J., Nikkinen, J., Tervonen, O., Kiviniemi, V., 2010. The effect of model order selection in group PICA. *Hum Brain Mapp* 31, 1207-1216.
- Achard, S., Bullmore, E., 2007. Efficiency and cost of economical brain functional networks. *Plos Comput Biol* 3, e17.
- Allen, E.A., Damaraju, E., Plis, S.M., Erhardt, E.B., Eichele, T., Calhoun, V.D., 2014. Tracking Whole-Brain Connectivity Dynamics in the Resting State. *Cereb Cortex* 24, 663-676.
- Allen, E.A., Erhardt, E.B., Damaraju, E., Gruner, W., Segall, J.M., Silva, R.F., Havlicek, M., Rachakonda, S., Fries, J., Kalyanam, R., Michael, A.M., Caprihan, A., Turner, J.A., Eichele, T., Adelsheim, S., Bryan, A.D., Bustillo, J., Clark, V.P., Feldstein Ewing, S.W., Filbey, F., Ford, C.C., Hutchison, K., Jung, R.E., Kiehl, K.A., Kodituwakku, P., Komesu, Y.M., Mayer, A.R., Pearlson, G.D., Phillips, J.P., Sadek, J.R., Stevens, M., Teuscher, U., Thoma, R.J., Calhoun, V.D., 2011. A baseline for the multivariate comparison of resting-state networks. *Front Syst Neurosci* 5, 2.
- Almeida, J.R.C., Versace, A., Hassel, S., Kupfer, D.J., Phillips, M.L., 2010. Elevated Amygdala Activity to Sad Facial Expressions: A State Marker of Bipolar but Not Unipolar Depression. *Biol Psychiatry* 67, 414-421.
- Anand, A., Li, Y., Wang, Y., Wu, J., Gao, S., Bukhari, L., Mathews, V.P., Kalnin, A., Lowe, M.J., 2005a. Activity and connectivity of brain mood regulating circuit in depression: a functional magnetic resonance study. *Biol Psychiatry* 57, 1079-1088.
- Anand, A., Li, Y., Wang, Y., Wu, J., Gao, S., Bukhari, L., Mathews, V.P., Kalnin, A., Lowe, M.J., 2005b. Antidepressant effect on connectivity of the mood-regulating circuit: an fMRI study. *Neuropsychopharmacology* 30, 1334-1344.
- Arbabshirani, M.R., Kiehl, K.A., Pearlson, G.D., Calhoun, V.D., 2013. Classification of schizophrenia patients based on resting-state functional network connectivity. *Front Neurosci* 7, 133.
- Baxter, L.R., Jr., Schwartz, J.M., Phelps, M.E., Mazziotta, J.C., Guze, B.H., Selin, C.E., Gerner, R.H., Sumida, R.M., 1989. Reduction of prefrontal cortex glucose metabolism common to three types of depression. *Arch Gen Psychiat* 46, 243-250.
- Bell, A.J., Sejnowski, T.J., 1995. An information-maximization approach to blind separation and blind deconvolution. *Neural Comput* 7, 1129-1159.
- Bench, C.J., Friston, K.J., Brown, R.G., Scott, L.C., Frackowiak, R.S., Dolan, R.J., 1992. The anatomy of melancholia--focal abnormalities of cerebral blood flow in major depression. *Psychol Med* 22, 607-615.
- Benjamini, Y., Hochberg, Y., 1995. Controlling the False Discovery Rate - a Practical and Powerful Approach to Multiple Testing. *J Roy Stat Soc B Met* 57, 289-300.
- Bertocci, M.A., Bebeko, G.M., Mullin, B.C., Langenecker, S.A., Ladouceur, C.D., Almeida, J.R.C., Phillips, M.L., 2012. Abnormal anterior cingulate cortical activity during emotional n-back task performance distinguishes bipolar from unipolar depressed females. *Psychol Med* 42, 1417-1428.
- Brotman, M.A., Kassem, L., Reising, M.M., Guyer, A.E., Dickstein, D.P., Rich, B.A., Towbin, K.E., Pine, D.S., McMahon, F.J., Leibenluft, E., 2007. Parental diagnoses in youth with narrow phenotype bipolar disorder or severe mood dysregulation. *Am J Psychiatry* 164, 1238-1241.
- Calhoun, V.D., Adali, T., 2012. Multisubject independent component analysis of fMRI: a decade of intrinsic networks, default mode, and neurodiagnostic discovery. *IEEE Rev Biomed Eng* 5, 60-73.
- Calhoun, V.D., Adali, T., Pearlson, G.D., Pekar, J.J., 2001a. A method for making group inferences from functional MRI data using independent component analysis. *Hum Brain Mapp* 14, 140-151.
- Calhoun, V.D., Adali, T., Pearlson, G.D., Pekar, J.J., 2001b. Spatial and temporal independent component analysis of functional MRI data containing a pair of task-related waveforms. *Hum Brain Mapp* 13, 43-53.
- Calhoun, V.D., Sui, J., Kiehl, K., Turner, J., Allen, E., Pearlson, G., 2011. Exploring the psychosis functional connectome: aberrant intrinsic networks in schizophrenia and bipolar disorder. *Front Psychiatry* 2, 75.

- Cardoso de Almeida, J.R., Phillips, M.L., 2013. Distinguishing between unipolar depression and bipolar depression: current and future clinical and neuroimaging perspectives. *Biol Psychiatry* 73, 111-118.
- Cerullo, M.A., Eliassen, J.C., Smith, C.T., Fleck, D.E., Nelson, E.B., Strawn, J.R., Lamy, M., DelBello, M.P., Adler, C.M., Strakowski, S.M., 2014. Bipolar I disorder and major depressive disorder show similar brain activation during depression. *Bipolar Disord* 16, 703-712.
- Chepenik, L.G., Raffo, M., Hampson, M., Lacadie, C., Wang, F., Jones, M.M., Pittman, B., Skudlarski, P., Blumberg, H.P., 2010. Functional connectivity between ventral prefrontal cortex and amygdala at low frequency in the resting state in bipolar disorder. *Psychiat Res-Neuroim* 182, 207-210.
- Cooney, R.E., Joormann, J., Eugene, F., Dennis, E.L., Gotlib, I.H., 2010. Neural correlates of rumination in depression. *Cogn Affect Behav Ne* 10, 470-478.
- Cordes, D., Haughton, V.M., Arfanakis, K., Wendt, G.J., Turski, P.A., Moritz, C.H., Quigley, M.A., Meyerand, M.E., 2000. Mapping functionally related regions of brain with functional connectivity MR imaging. *AJNR Am J Neuroradiol* 21, 1636-1644.
- Craddock, R.C., Holtzheimer, P.E., 3rd, Hu, X.P., Mayberg, H.S., 2009. Disease state prediction from resting state functional connectivity. *Magnet Reson Med* 62, 1619-1628.
- Damaraju, E., Allen, E.A., Belger, A., Ford, J.M., McEwen, S., Mathalon, D.H., Mueller, B.A., Pearlson, G.D., Potkin, S.G., Preda, A., Turner, J.A., Vaidya, J.G., van Erp, T.G., Calhoun, V.D., 2014. Dynamic functional connectivity analysis reveals transient states of dysconnectivity in schizophrenia. *Neuroimage Clin* 5, 298-308.
- de Almeida, J.R.C., Versace, A., Mechelli, A., Hassel, S., Quevedo, K., Kupfer, D.J., Phillips, M.L., 2009. Abnormal Amygdala-Prefrontal Effective Connectivity to Happy Faces Differentiates Bipolar from Major Depression. *Biol Psychiatry* 66, 451-459.
- Dennis, E.L., Jahanshad, N., Toga, A.W., McMahon, K.L., de Zubicaray, G.I., Martin, N.G., Wright, M.J., Thompson, P.M., 2012. Test-retest reliability of graph theory measures of structural brain connectivity. *Med Image Comput Comput Assist Interv* 15, 305-312.
- Diler, R.S., de Almeida, J.R.C., Ladouceur, C., Birmaher, B., Axelson, D., Phillips, M., 2013. Neural activity to intense positive versus negative stimuli can help differentiate bipolar disorder from unipolar major depressive disorder in depressed adolescents: A pilot fMRI study. *Psychiat Res-Neuroim* 214, 277-284.
- Drevets, W.C., 2000. Neuroimaging studies of mood disorders. *Biol Psychiatry* 48, 813-829.
- Drevets, W.C., 2001. Neuroimaging and neuropathological studies of depression: implications for the cognitive-emotional features of mood disorders. *Curr Opin Neurobiol* 11, 240-249.
- Du, Y.H., Fan, Y., 2013. Group information guided ICA for fMRI data analysis. *Neuroimage* 69, 157-197.
- Du, Y.H., Li, H.M., Wu, H., Fan, Y., 2012. Identification of subject specific and functional consistent ROIs using semi-supervised learning. *Medical Imaging 2012: Image Processing* 8314.
- Dudek, D., Siwek, M., Zielinska, D., Jaeschke, R., Rybakowski, J., 2013. Diagnostic conversions from major depressive disorder into bipolar disorder in an outpatient setting: results of a retrospective chart review. *J Affect Disord* 144, 112-115.
- Erhardt, E.B., Rachakonda, S., Bedrick, E.J., Allen, E.A., Adali, T., Calhoun, V.D., 2011. Comparison of multi-subject ICA methods for analysis of fMRI data. *Hum Brain Mapp* 32, 2075-2095.
- Foland, L.C., Altshuler, L.L., Bookheimer, S.Y., Eisenberger, N., Townsend, J., Thompson, P.M., 2008. Evidence for deficient modulation of amygdala response by prefrontal cortex in bipolar mania. *Psychiatry Res* 162, 27-37.
- Freire, L., Roche, A., Mangin, J.F., 2002. What is the best similarity measure for motion correction in fMRI time series? *IEEE Trans Med Imaging* 21, 470-484.
- Friston, K.J., 2002. Beyond phrenology: What can neuroimaging tell us about distributed circuitry? *Annu Rev Neurosci* 25, 221-250.
- Grotegerd, D., Stuhmann, A., Kugel, H., Schmidt, S., Redlich, R., Zwanzger, P., Rauch, A.V., Heindel, W., Zwieterlood, P., Arolt, V., Suslow, T., Dannlowski, U., 2014. Amygdala excitability to subliminally

- presented emotional faces distinguishes unipolar and bipolar depression: an fMRI and pattern classification study. *Hum Brain Mapp* 35, 2995-3007.
- He, H., Sui, J., Yu, Q., Turner, J.A., Ho, B.C., Sponheim, S.R., Manoach, D.S., Clark, V.P., Calhoun, V.D., 2012. Altered small-world brain networks in schizophrenia patients during working memory performance. *PLoS One* 7, e38195.
- Hirschfeld, R.M., Lewis, L., Vornik, L.A., 2003. Perceptions and impact of bipolar disorder: how far have we really come? Results of the national depressive and manic-depressive association 2000 survey of individuals with bipolar disorder. *J Clin Psychiatry* 64, 161-174.
- Hirschfeld, R.M.A., Vornik, L.A., 2005. Bipolar disorder - Costs and comorbidity. *American Journal of Managed Care* 11, S85-S90.
- Jafri, M.J., Pearlson, G.D., Stevens, M., Calhoun, V.D., 2008. A method for functional network connectivity among spatially independent resting-state components in schizophrenia. *Neuroimage* 39, 1666-1681.
- Jie, N., Zhu, M., Ma, X., Osuch, E.A., Wammes, M., Théberge, J., Li, H., Zhang, Y., Jiang, T., Sui, J., Calhoun, V.D., 2015. Discriminating Bipolar Disorder From Major Depression Based on SVM-FoBa: Efficient Feature Selection With Multimodal Brain Imaging Data. *IEEE Transactions on Autonomous Mental Development* In press.
- Johnson, S.L., McKenzie, G., McMurrich, S., 2008. Ruminative Responses to Negative and Positive Affect Among Students Diagnosed with Bipolar Disorder and Major Depressive Disorder. *Cognitive Ther Res* 32, 702-713.
- Judd, L.L., Akiskal, H.S., Schettler, P.J., Coryell, W., Endicott, J., Maser, J.D., Solomon, D.A., Leon, A.C., Keller, M.B., 2003. A prospective investigation of the natural history of the long-term weekly symptomatic status of bipolar II disorder. *Arch Gen Psychiat* 60, 261-269.
- Judd, L.L., Akiskal, H.S., Schettler, P.J., Endicott, J., Maser, J., Solomon, D.A., Leon, A.C., Rice, J.A., Keller, M.B., 2002. The long-term natural history of the weekly symptomatic status of bipolar I disorder. *Arch Gen Psychiat* 59, 530-537.
- Kaiser, M., Hilgetag, C.C., 2004. Modelling the development of cortical systems networks. *Computational Neuroscience: Trends in Research* 2004, 297-302.
- Kiviniemi, V., Kantola, J.H., Jauhiainen, J., Hyvarinen, A., Tervonen, O., 2003. Independent component analysis of nondeterministic fMRI signal sources. *Neuroimage* 19, 253-260.
- Kiviniemi, V., Starck, T., Remes, J., Long, X., Nikkinen, J., Haapea, M., Veijola, J., Moilanen, I., Isohanni, M., Zang, Y.F., Tervonen, O., 2009. Functional segmentation of the brain cortex using high model order group PICA. *Hum Brain Mapp* 30, 3865-3886.
- Kupfer, D.J., 2005. The increasing medical burden in bipolar disorder. *Jama* 293, 2528-2530.
- Kupfer, D.J., Frank, E., Phillips, M.L., 2012. Major depressive disorder: new clinical, neurobiological, and treatment perspectives. *Lancet* 379, 1045-1055.
- Latora, V., Marchiori, M., 2001. Efficient behavior of small-world networks. *Phys Rev Lett* 87.
- Lynall, M.E., Bassett, D.S., Kerwin, R., McKenna, P.J., Kitzbichler, M., Muller, U., Bullmore, E., 2010. Functional connectivity and brain networks in schizophrenia. *J Neurosci* 30, 9477-9487.
- McKeown, M.J., Makeig, S., Brown, G.G., Jung, T.P., Kindermann, S.S., Bell, A.J., Sejnowski, T.J., 1998. Analysis of fMRI data by blind separation into independent spatial components. *Hum Brain Mapp* 6, 160-188.
- McKeown, M.J., Sejnowski, T.J., 1998. Independent component analysis of fMRI data: examining the assumptions. *Hum Brain Mapp* 6, 368-372.
- Montgomery, S.A., Asberg, M., 1979. New Depression Scale Designed to Be Sensitive to Change. *Brit J Psychiat* 134, 382-389.
- Murray, C.J.L., Lopez, A.D., World Health Organization., World Bank., Harvard School of Public Health., 1996. The Global burden of disease : a comprehensive assessment of mortality and disability from diseases, injuries, and risk factors in 1990 and projected to 2020. World Health Organization, Geneva.

- Ongur, D., Lundy, M., Greenhouse, I., Shinn, A.K., Menon, V., Cohen, B.M., Renshaw, P.F., 2010. Default mode network abnormalities in bipolar disorder and schizophrenia. *Psychiatry Res* 183, 59-68.
- Passarotti, A.M., Ellis, J., Wegbreit, E., Stevens, M.C., Pavuluri, M.N., 2012. Reduced functional connectivity of prefrontal regions and amygdala within affect and working memory networks in pediatric bipolar disorder. *Brain Connect* 2, 320-334.
- Pavuluri, M.N., O'Connor, M.M., Harral, E., Sweeney, J.A., 2007. Affective neural circuitry during facial emotion processing in pediatric bipolar disorder. *Biol Psychiatry* 62, 158-167.
- Pavuluri, M.N., O'Connor, M.M., Harral, E.M., Sweeney, J.A., 2008. An fMRI study of the interface between affective and cognitive neural circuitry in pediatric bipolar disorder. *Psychiat Res-Neuroim* 162, 244-255.
- Phillips, M.L., Ladouceur, C.D., Drevets, W.C., 2008. A neural model of voluntary and automatic emotion regulation: implications for understanding the pathophysiology and neurodevelopment of bipolar disorder. *Mol Psychiatr* 13, 829, 833-857.
- Power, J.D., Barnes, K.A., Snyder, A.Z., Schlaggar, B.L., Petersen, S.E., 2012. Spurious but systematic correlations in functional connectivity MRI networks arise from subject motion (vol 59, pg 2142, 2012). *Neuroimage* 63, 999-999.
- Price, J.L., Drevets, W.C., 2012. Neural circuits underlying the pathophysiology of mood disorders. *Trends Cogn Sci* 16, 61-71.
- Raffo, M., Hampson, M., Lacadie, C., Jones, M., Skudlarski, P., Constable, R.T., Krystal, J.H., Blumberg, H.P., 2004. Functional connectivity between ventral prefrontal cortex and amygdala in bipolar disorder. *Biol Psychiatry* 55, 229s-229s.
- Rubinov, M., Sporns, O., 2010. Complex network measures of brain connectivity: uses and interpretations. *Neuroimage* 52, 1059-1069.
- Spencer, K.M., Nestor, P.G., Perlmuter, R., Niznikiewicz, M.A., Klump, M.C., Frumin, M., Shenton, M.E., McCarley, R.W., 2004. Neural synchrony indexes disordered perception and cognition in schizophrenia. *Proc Natl Acad Sci U S A* 101, 17288-17293.
- Sporns, O., 2011. *Networks of the brain*. MIT Press, Cambridge, Mass. ; London.
- Stein, J.L., Wiedholz, L.M., Bassett, D.S., Weinberger, D.R., Zink, C.F., Mattay, V.S., Meyer-Lindenberg, A., 2007. A validated network of effective amygdala connectivity. *Neuroimage* 36, 736-745.
- Strakowski, S.M., Adler, C.M., Almeida, J., Altshuler, L.L., Blumberg, H.P., Chang, K.D., DelBello, M.P., Frangou, S., McIntosh, A., Phillips, M.L., Sussman, J.E., Townsend, J.D., 2012. The functional neuroanatomy of bipolar disorder: a consensus model. *Bipolar Disord* 14, 313-325.
- Sui, J., Adali, T., Pearlson, G.D., Calhoun, V.D., 2009. An ICA-based method for the identification of optimal FMRI features and components using combined group-discriminative techniques. *Neuroimage* 46, 73-86.
- Sui, J., Adali, T., Yu, Q., Chen, J., Calhoun, V.D., 2012. A review of multivariate methods for multimodal fusion of brain imaging data. *J Neurosci Meth* 204, 68-81.
- Sui, J., Huster, R., Yu, Q., Segall, J.M., Calhoun, V.D., 2014. Function-structure associations of the brain: evidence from multimodal connectivity and covariance studies. *Neuroimage* 102 Pt 1, 11-23.
- Sui, J., Pearlson, G., Caprihan, A., Adali, T., Kiehl, K.A., Liu, J., Yamamoto, J., Calhoun, V.D., 2011. Discriminating schizophrenia and bipolar disorder by fusing fMRI and DTI in a multimodal CCA+ joint ICA model. *Neuroimage* 57, 839-855.
- Sui, J., Pearlson, G.D., Du, Y., Yu, Q., Jones, T.R., Chen, J., Jiang, T., Bustillo, J., Calhoun, V.D., 2015. In *Search of Multimodal Neuroimaging Biomarkers of Cognitive Deficits in Schizophrenia*. *Biol Psychiatry*.
- Tang, Y., Kong, L., Wu, F., Womer, F., Jiang, W., Cao, Y., Ren, L., Wang, J., Fan, G., Blumberg, H.P., Xu, K., Wang, F., 2013. Decreased functional connectivity between the amygdala and the left ventral prefrontal cortex in treatment-naïve patients with major depressive disorder: a resting-state functional magnetic resonance imaging study. *Psychol Med* 43, 1921-1927.

- Taylor Tavares, J.V., Clark, L., Furey, M.L., Williams, G.B., Sahakian, B.J., Drevets, W.C., 2008. Neural basis of abnormal response to negative feedback in unmedicated mood disorders. *Neuroimage* 42, 1118-1126.
- Van Dijk, K.R., Hedden, T., Venkataraman, A., Evans, K.C., Lazar, S.W., Buckner, R.L., 2010. Intrinsic functional connectivity as a tool for human connectomics: theory, properties, and optimization. *J Neurophysiol* 103, 297-321.
- Van Dijk, K.R., Sabuncu, M.R., Buckner, R.L., 2012. The influence of head motion on intrinsic functional connectivity MRI. *Neuroimage* 59, 431-438.
- Varela, F., Lachaux, J.P., Rodriguez, E., Martinerie, J., 2001. The brainweb: phase synchronization and large-scale integration. *Nat Rev Neurosci* 2, 229-239.
- Veer, I.M., Beckmann, C.F., van Tol, M.J., Ferrarini, L., Milles, J., Veltman, D.J., Aleman, A., van Buchem, M.A., van der Wee, N.J., Rombouts, S.A., 2010. Whole brain resting-state analysis reveals decreased functional connectivity in major depression. *Front Syst Neurosci* 4.
- Wang, L., Hermens, D.F., Hickie, I.B., Lagopoulos, J., 2012. A systematic review of resting-state functional-MRI studies in major depression. *J Affect Disord* 142, 6-12.
- Wang, L., Metzak, P.D., Honer, W.G., Woodward, T.S., 2010. Impaired efficiency of functional networks underlying episodic memory-for-context in schizophrenia. *J Neurosci* 30, 13171-13179.
- Watts, D.J., Strogatz, S.H., 1998. Collective dynamics of 'small-world' networks. *Nature* 393, 440-442.
- Xia, M., Wang, J., He, Y., 2013. BrainNet Viewer: a network visualization tool for human brain connectomics. *PLoS One* 8, e68910.
- Yan, C.G., Craddock, R.C., He, Y., Milham, M.P., 2013. Addressing head motion dependencies for small-world topologies in functional connectomics. *Front Hum Neurosci* 7.
- Young, R.C., Biggs, J.T., Ziegler, V.E., Meyer, D.A., 1978. A rating scale for mania: reliability, validity and sensitivity. *Br J Psychiatry* 133, 429-435.
- Yu, Q., Sui, J., Rachakonda, S., He, H., Gruner, W., Pearlson, G., Kiehl, K.A., Calhoun, V.D., 2011a. Altered topological properties of functional network connectivity in schizophrenia during resting state: a small-world brain network study. *PLoS One* 6, e25423.
- Yu, Q., Sui, J., Rachakonda, S., He, H., Pearlson, G., Calhoun, V.D., 2011b. Altered small-world brain networks in temporal lobe in patients with schizophrenia performing an auditory oddball task. *Front Syst Neurosci* 5, 7.
- Zhu, X., Wang, X., Xiao, J., Liao, J., Zhong, M., Wang, W., Yao, S., 2012. Evidence of a dissociation pattern in resting-state default mode network connectivity in first-episode, treatment-naïve major depression patients. *Biol Psychiatry* 71, 611-617.

Highlights

- BD showed more closely connected and efficient functional structures than MDD
- Differences in FNC between BD and MDD were found largely within PFC networks
- More severely depressed patients manifested lower interconnection in PFC networks
- BD exhibited higher clustered FNC in default-mode networks compared to HC
- The difference in FNC between MDD and HC was not significant after FDR correction